Neutronic Performance of LWTS Moderators
Configuration LW1K32
LWTS-6001-RE-A-00

E. B. Iverson

3 October 2000

This document summarizes the neutronic performance characteristics predicted for the moderators suggested for the Long-Wavelength Target Station (LWTS). All predictions are normalized on the basis of "per proton pulse," in which each proton pulse is 34 kJ of 1 GeV protons on LWTS.

1 Model Description

The LWTS configuration used for these comparisons is denoted LW1K32. Although this configuration represents our current state, our design is rapidly changing. These predictions should be considered to represent a target station best described as a partially-optimized work-in-progress. As the target station design evolves, this document will evolve to reflect changes in performance. Configuration LW1K32 includes three moderators, of which two are "slab" moderators and one is a "front wing" moderator. Each of these moderators is viewed from one side only. All moderators have nominal viewed faces of 120 mm (horizontal) by 200 mm (vertical). The reflector (out to a radius of $\approx$500 mm) is beryllium and is cooled with heavy water. This reflector is surrounded by a shield of iron cooled heavy water. Table 1 summarizes relevant characteristics of the target station configuration used for this set of calculations. Although nominal operation is considered to be at 10 Hz (and thus 340 kW), the actual repetition rate has yet to be

Proton Energy	1 GeV
Pulse Rate	10 Hz
Average Power	340 kW
Energy per pulse	34 kJ
Proton Beam Shape	rectangular
Proton Beam Size	50x150 mm^2
Proton Pulse	$\delta(t)$
Target	W
Inner Reflector	Be
I.R. Coolant	D_2O
Outer Reflector	Be
O.R. Coolant	D_2O

Table 1: LWTS parameters used in calculations. All normalizations are performed per 34 kJ-pulse.

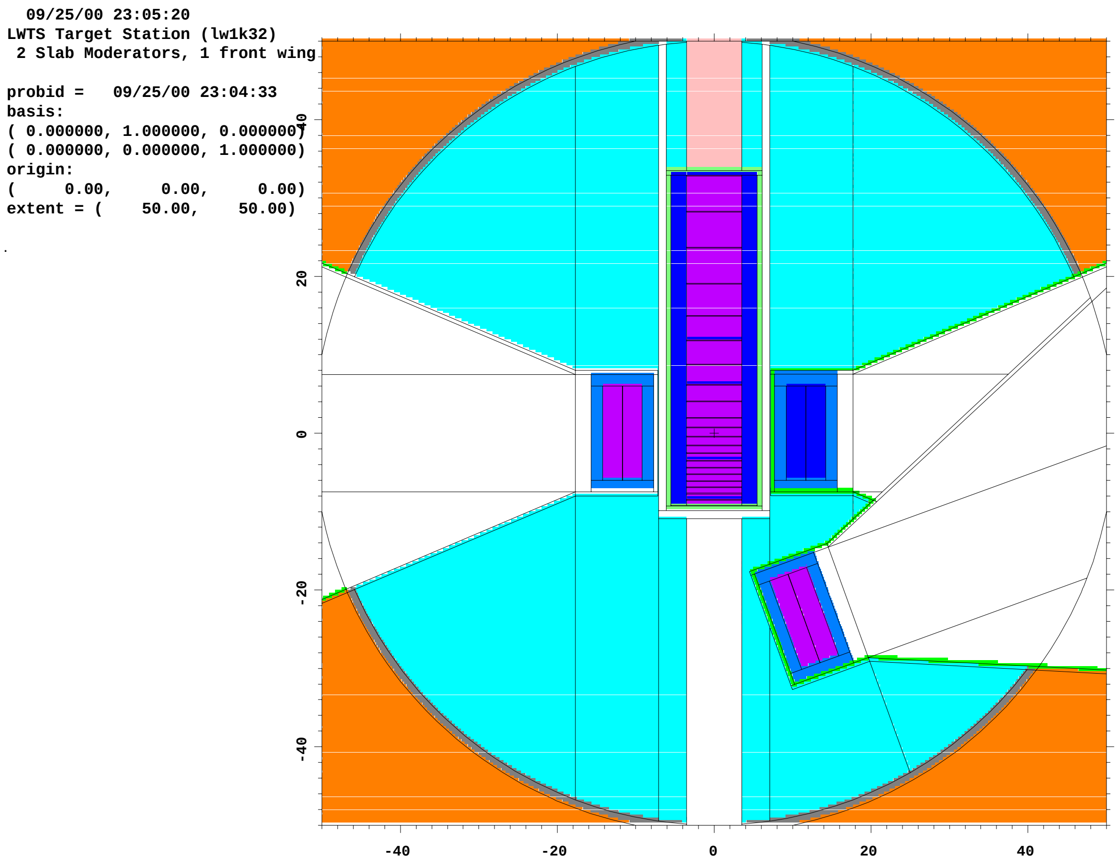

Figure 1: Top view LWTS moderator and target layout. The moderators to the right of the target are decoupled. The left slab moderator and the front wing moderator are solid methane. Protons enter from the bottom of the figure. Dimensions are in centimeters.

determined; 34 kJ per pulse is the value to be considered constant. Figure 1 shows the general layout of target and moderators for this LWTS configuration.

The “port slab” moderator is the slab moderator to the left of the target, when viewed from the direction of the incoming proton beam. This moderator is fully coupled to the reflector, and is composed of solid methane at 22 K (90% by volume) and aluminum (10% by volume). The “starboard slab” moderator is the slab moderator to the right of the target, when viewed from the direction of the incoming proton beam. This moderator is decoupled from the reflector with cadmium, is composed of liquid methane at 100 K and is poisoned with gadolinium 25 mm beneath the viewed surface. The “front wing” moderator is upstream (for the proton beam) of the target, decoupled with cadmium, poisoned with gadolinium, and composed of solid methane at 22 K K (90% by volume) and aluminum (10% by volume). All moderators are 120 mm (horizontal) by 200 mm (vertical) by 50 mm (depth). Table 2 summarizes this moderator configuration. Note that in our current judgment, all slab moderators must be viewed indirectly, i.e., through a curved guide or compact beam bender.

ID Code	Moderator Location	Moderator Material	Temperature (K)	Decoupling Material	Poison Material	Poison Depth (mm)
source_lw1k32_cosmsl	Port Slab	CH_4	22	–	–	–
source_lw1k32_delmsl	Starboard Slab	CH_4	100	Cd	Gd	25
source_lw1k32_desmfw	Front Wing	CH_4	22	Cd	Gd	25

Table 2: LWTS moderator summary. Solid methane is diluted with aluminum at 10% by volume.

1.1 Variant Design

Our current prediction is that we will switch the two decoupled moderators with each other, i.e., the front wing will become liquid methane and the starboard slab will become solid methane. In general, we could assume that the spectral shape for a decoupled moderator would depend on the moderator material, while the overall scale would depend upon the position, at least for the controlled substitution here. Such a substitution would, in this case, result in the liquid methane spectrum, which would be available from the front wing moderator, being scaled down by a factor of roughly 2.8, while the solid methane spectrum, which would be available from the slab moderator through an indirect beam-line, would be scaled up by that same factor of 2.8. Conventionally, we would anticipate that this change in scale would take place without any changes in the shape of the emission time distributions, e.g., the liquid methane pulse shape would remain unchanged regardless of moderator position; only the overall scale would shift. Source files which employ this scale factor to estimate this variant design are available along with source files for the base design (see below). However, these source files will not properly account for the behavior described in the next paragraph.

Our current model indicates a somewhat unexpected change in pulse shape between the current front wing moderator and the remaining moderators. Figure 2 shows that the solid methane front wing moderator emission time distribution at high (slowing-down) energies is somewhat different when compared to either slab moderator (the relative height in the "tail" is greater). We would conventionally expect all these moderators to have nearly identical slowing-down properties, as the proton density in liquid methane and in the solid methane-aluminum mix is very similar. Although this difference appears rather small, and does not significantly influence, for example, the Full-Width-Half-Maximum of the pulse shape (see Figure 4(b)), the difference does result in an RMS deviation significantly (45%) larger for this front wing moderator. Although this effect is small by some metrics, if one wishes to use the source files described as the variant design, one should keep the effect in mind.

2 Quantities Calculated

The spectral intensity $i(E)$ of a moderator is a measure of the number of neutrons leaving the moderator at a particular energy E, and is related to the differential flux $\phi(E)$ at a point some large distance L from the moderator by

$$i(E) = L^2 \left. \phi(E) \right|_L , \tag{1}$$

where the flight path is normal to the viewed moderator face. This intensity is thus independent of flight path length. If the flight path is not normal to the moderator surface, the intensity observed is scaled by the cosine of the angle between the flight path and the normal to the moderator surface. The intensity is usually separated into a shape and an overall scale factor, with the overall scale factor equal to the intensity evaluated at 1 eV, referred to as the "moderator coupling,"

$$I_\mathrm{e} = \left. E i(E) \right|_{1\mathrm{eV}} , \tag{2}$$

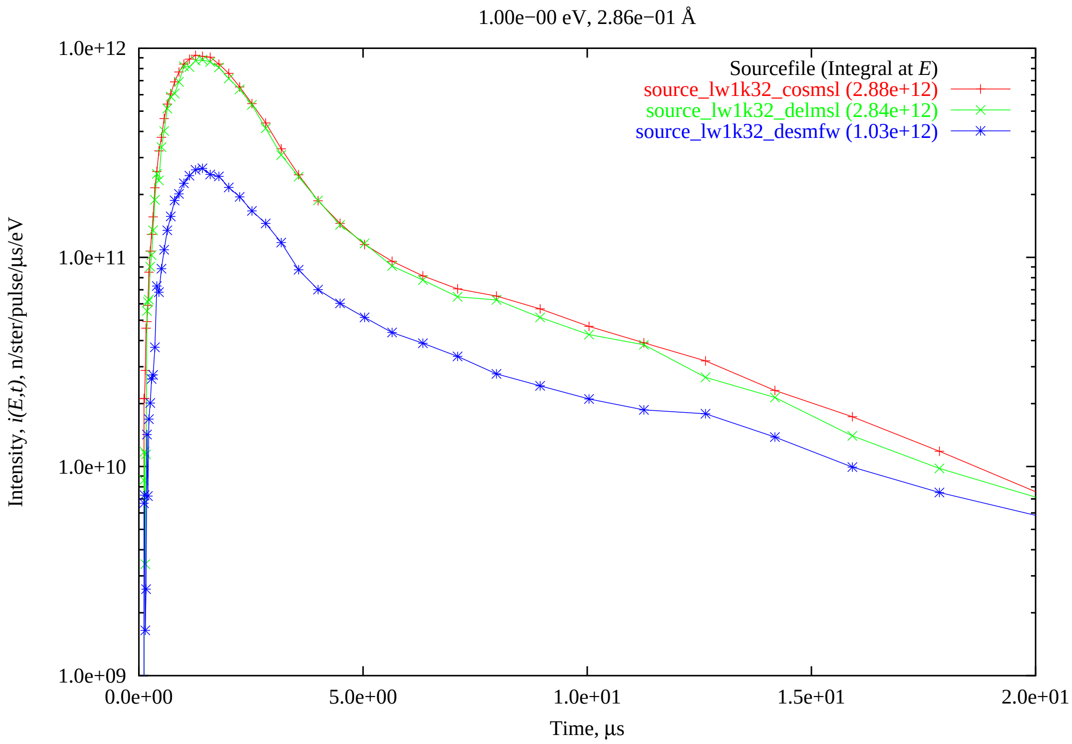

Figure 2: Emission time distribution for 1 eV neutrons. The coupled moderator is denoted source_lw1k32_cosmsl, the decoupled liquid methane slab moderator source_lw1k32_delmsl, and the decoupled solid methane front wing moderator source_lw1k32_desmfw. $\Delta E/E \approx 23$ %.

or the epithermal flux. Note that slab moderators are assumed to require indirect views of the moderator, and thus 1 eV neutrons would likely not be available from those moderators; we nonetheless use I_{e} as a metric for characterizing the moderator performance. The previously-mentioned factor of 2.8 between the slab and front wing decoupled moderator locations expresses through this I_{e}.

The emission time distribution of the moderator, also called the pulse shape, is simply the intensity distribution as a function of the time (after the initial proton pulse strikes the target) at which neutrons cross the moderator surface,

$$i(E) = \int_0^\infty i(E,t)dt. \qquad (3)$$

The emission time distribution of the neutrons leaving the moderator is dependent upon the viewing angle only in the scaling of the overall intensity. The energy binning and time binning for the Monte Carlo calculations provide 10 energy bins and 20 time bins per decade, such that $\Delta E/E \approx 23$ % and $\Delta t/t \approx 11$ %. The predictions reported are differential values averaged over such bins.

3 Calculational Techniques

The simulations reported are the results of calculations using the MCNPX code (version 2.1.5) and the Lahet Code System, both from LANL. The spectral intensities shown result from calculations using tallies at point detectors located 5 m from the viewed surface of the moderators. The emission time distributions (pulse shapes) come from current tallies on the viewed surface of the moderator material, and are averaged over 2π steradians. Weight windows used to accelerate the pulse shape calculations were generated by separate iterative runs using MCNP 4B in parallel mode on a large cluster of machines with a neutron-only source term. Coupled Lahet-MCNP 4B calculations produced the final results. The emission time distributions have been scaled (from the point detector calculations) to correspond to the intensity coming off of the moderator face in the normal direction, rather than the average over 2π steradians. Each moderator nominally requires a unique set of weight windows, and thus a unique set of runs. In some runs, however, the results for moderators other than the one for which the weight windows were optimized are adequately sampled.

The data exhibit minor anomalies that result from the methods of calculation. The step in the intensity spectra around 1 eV arises from the transition from atomic scattering cross sections to molecular scattering kernels. Jagged behavior at low energies is partly due to computational statistics (see below regarding extrapolation) and partly due to coarse discretization in the representation of the scattering kernel used by the code. Irregularities in the RMS emission time are due to calculational statistics.

4 Extrapolation

The results of the various simulations are reported, both here and in the source files, over a broad range of energies. In the event that results for energies outside this range are desired, certain extrapolations are reasonable. Spectra can be extrapolated to higher energies by using a simple power law, as they are very nearly, but not exactly, $1/E$ up to energies of approximately 100 keV. Emission time distributions for higher energies (in the slowing-down region) can in general be assumed to be invariant as a function of vt (velocity multiplied by time), equivalent to t/λ. However, the proton pulse at SNS is not actually a delta function in time, but rather has a width of a few hundred nanoseconds. Neutron pulse shapes for energies above 3 eV or so will be influenced by this proton pulse shape, while neutron pulse shapes for energies above 40 eV or so will be completely dominated by the proton pulse shape, and thus will be invariant as a function of time. At low energies, the spectral intensity from water or methane moderators can be assumed to follow a Maxwellian distribution in the low-energy limit, while the pulse shape is roughly invariant in time. The low-energy intensity from composite or hydrogen moderators can be extrapolated with a power law relationship from the data shown, and will likely not correspond to a Maxwellian distribution.

5 Data Availability

These results are available electronically as “source files;” ASCII files containing the spectra and emission time distributions, with comments showing the file format. Each moderator is represented by a single source file, the names of which are based on the indicated ID codes. These source files and many others can be downloaded from http://www.sns.anl.gov under “R&D Projects.”

6 Detailed Pulse Shapes

The detailed pulse shapes as produced by the simulations appear below. These data are completely un-processed, and appear exactly as they result from the calculations. The results are for the different moderators as described in Table 2. Recall that slab moderators must be viewed indirectly, implying a cut-off wavelength below which neutrons are unavailable due to the characteristics of the viewing optics.

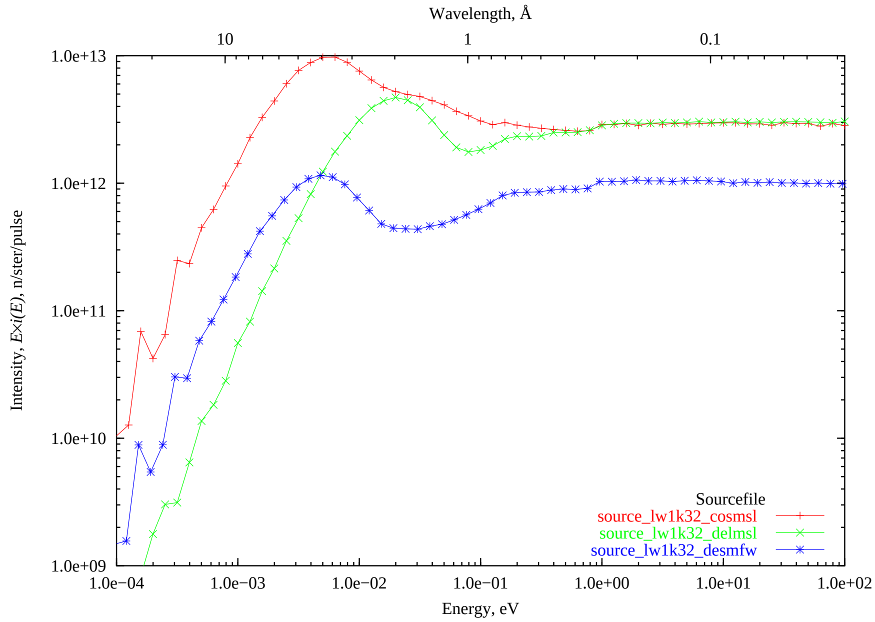

(a) Intensity

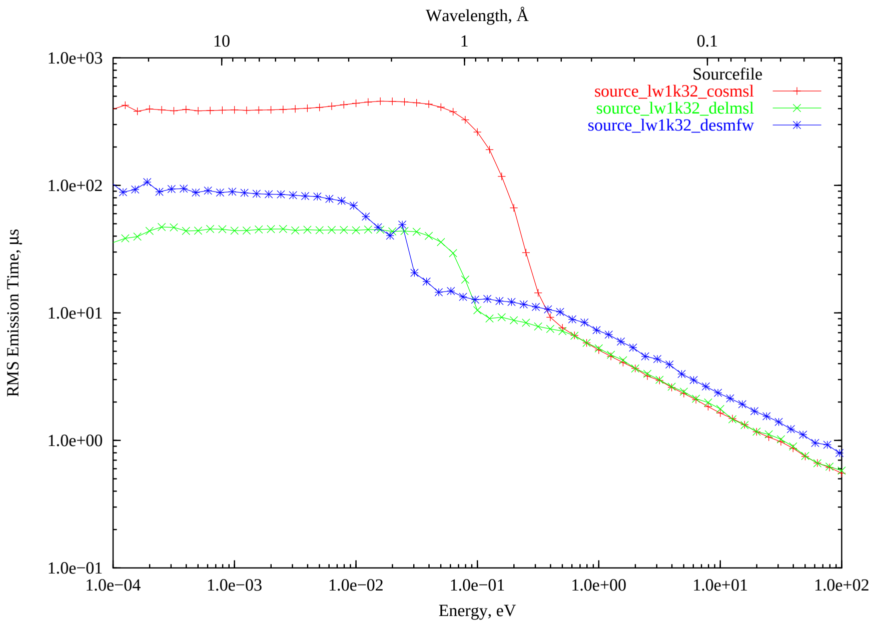

(b) Pulse Width (RMS)

Figure 3: Intensity (per unit lethargy) and pulse widths (RMS) as functions of energy for compared moderators. Recall that slab moderators must be indirectly viewed. The coupled moderator is denoted source_lw1k32_cosmsl, the decoupled liquid methane slab moderator source_lw1k32_delmsl, and the decoupled solid methane front wing moderator source_lw1k32_desmfw.

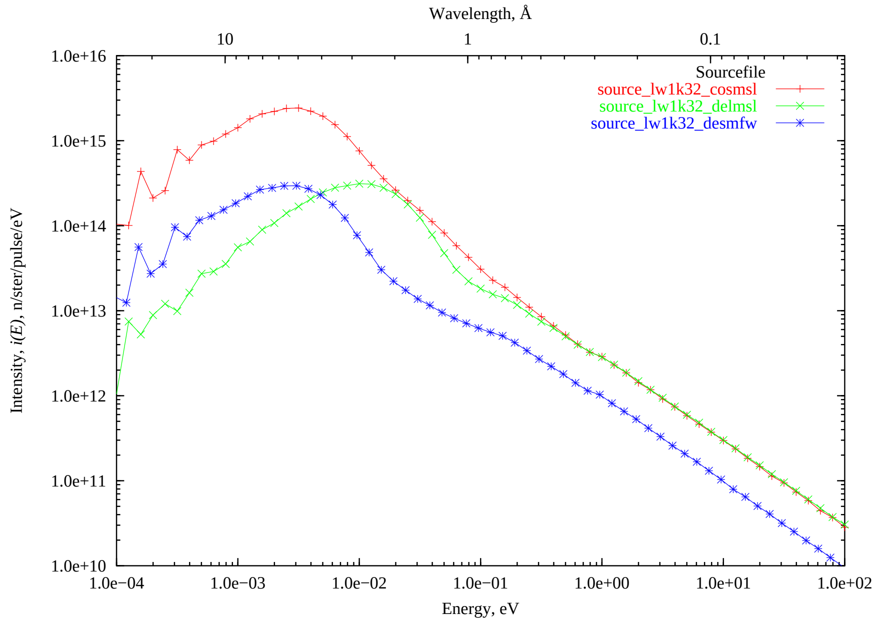

(a) Intensity

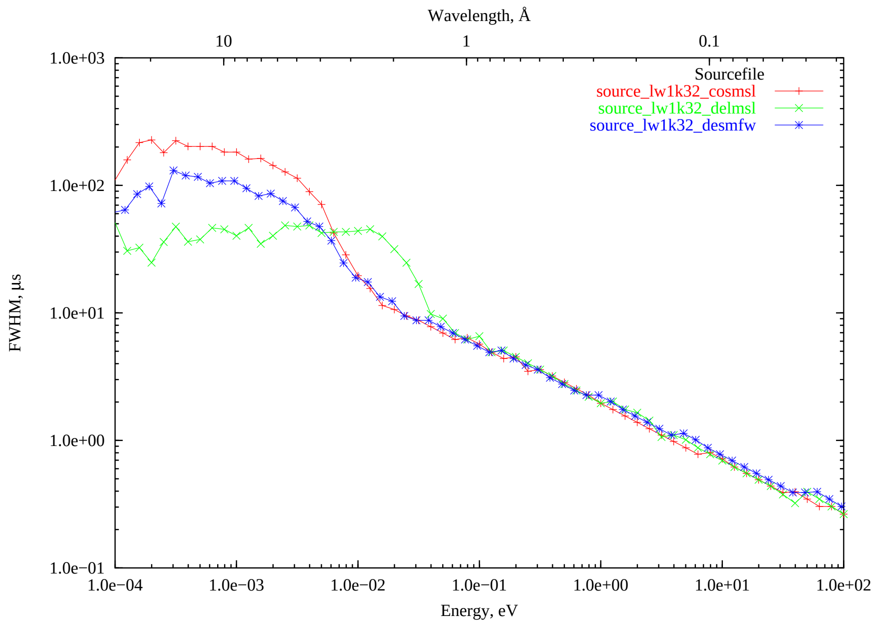

(b) Pulse Width (FWHM)

Figure 4: Intensity (per unit lethargy) and pulse widths (FWHM) as functions of energy for compared moderators. Recall that slab moderators must be indirectly viewed. The coupled moderator is denoted source_lw1k32_cosmsl, the decoupled liquid methane slab moderator source_lw1k32_delmsl, and the decoupled solid methane front wing moderator source_lw1k32_desmfw.

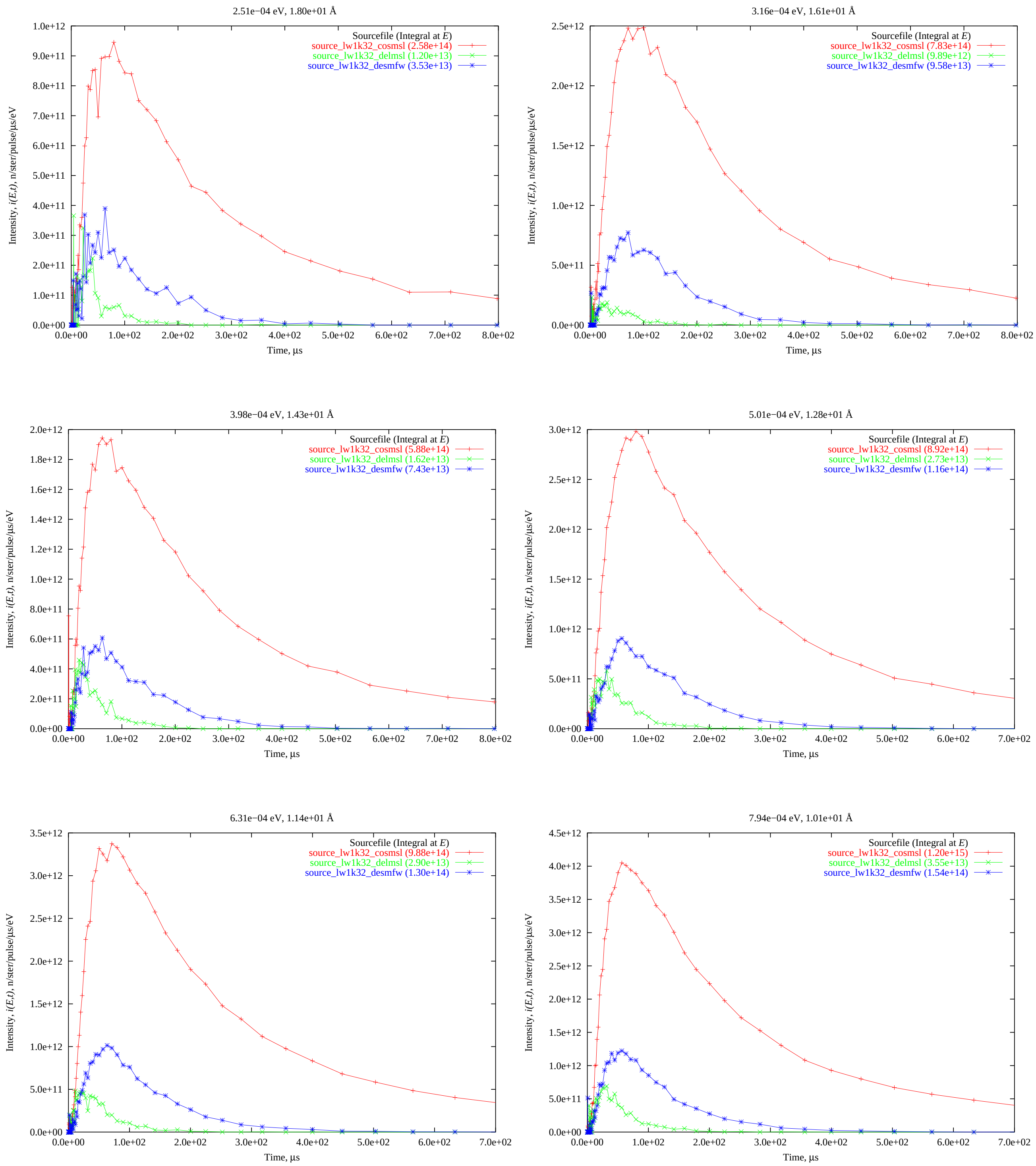

Figure 5: Emission time distributions. The coupled moderator is denoted source_lw1k32_cosmsl, the decoupled liquid methane slab moderator source_lw1k32_delmsl, and the decoupled solid methane front wing moderator source_lw1k32_desmfw. $\Delta E/E \approx 23$ %. Recall that slab moderators must be viewed indirectly.

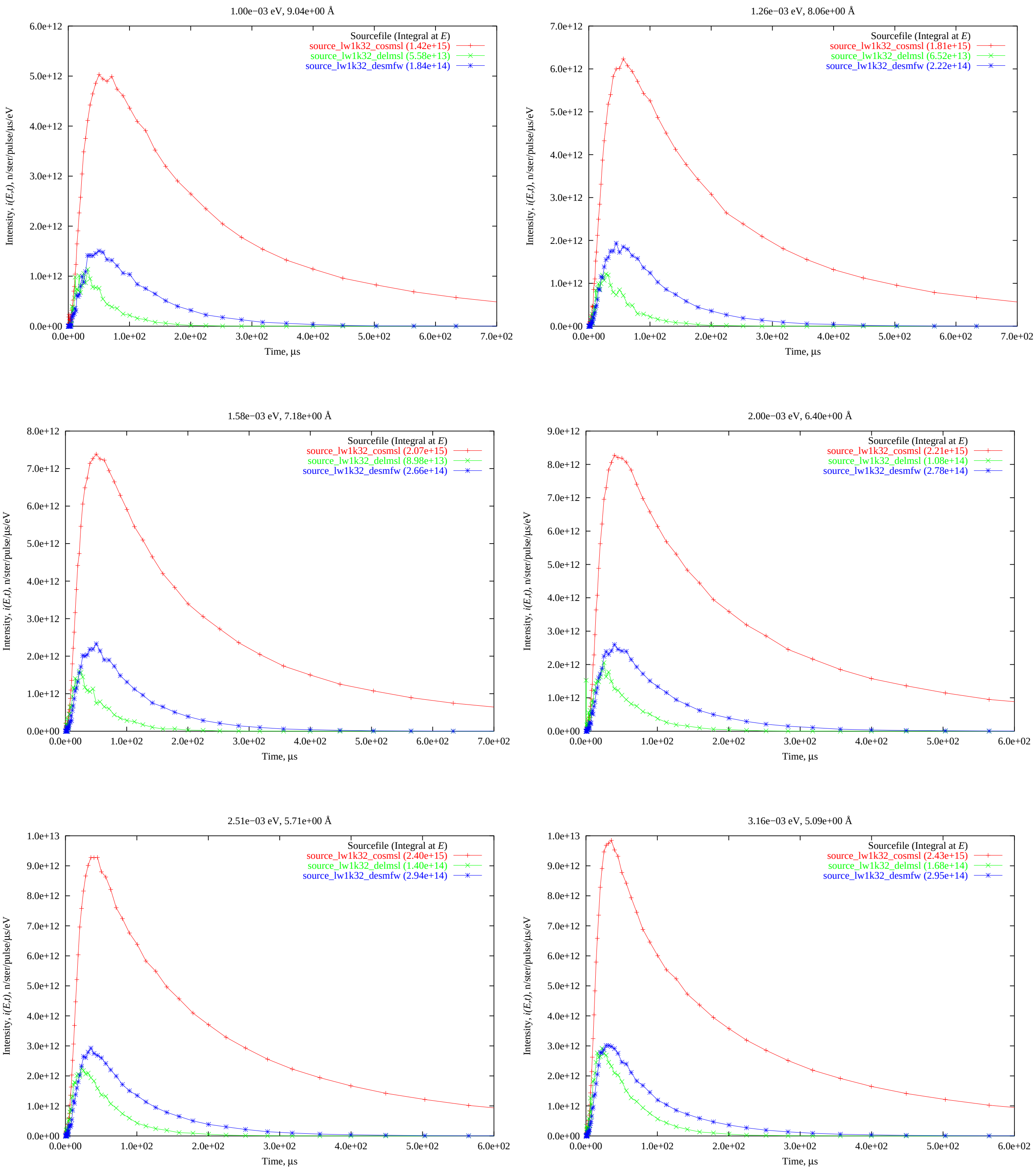

Figure 6: Emission time distributions. The coupled moderator is denoted source_lw1k32_cosmsl, the decoupled liquid methane slab moderator source_lw1k32_delmsl, and the decoupled solid methane front wing moderator source_lw1k32_desmfw. $\Delta E/E \approx 23$ %. Recall that slab moderators must be viewed indirectly.

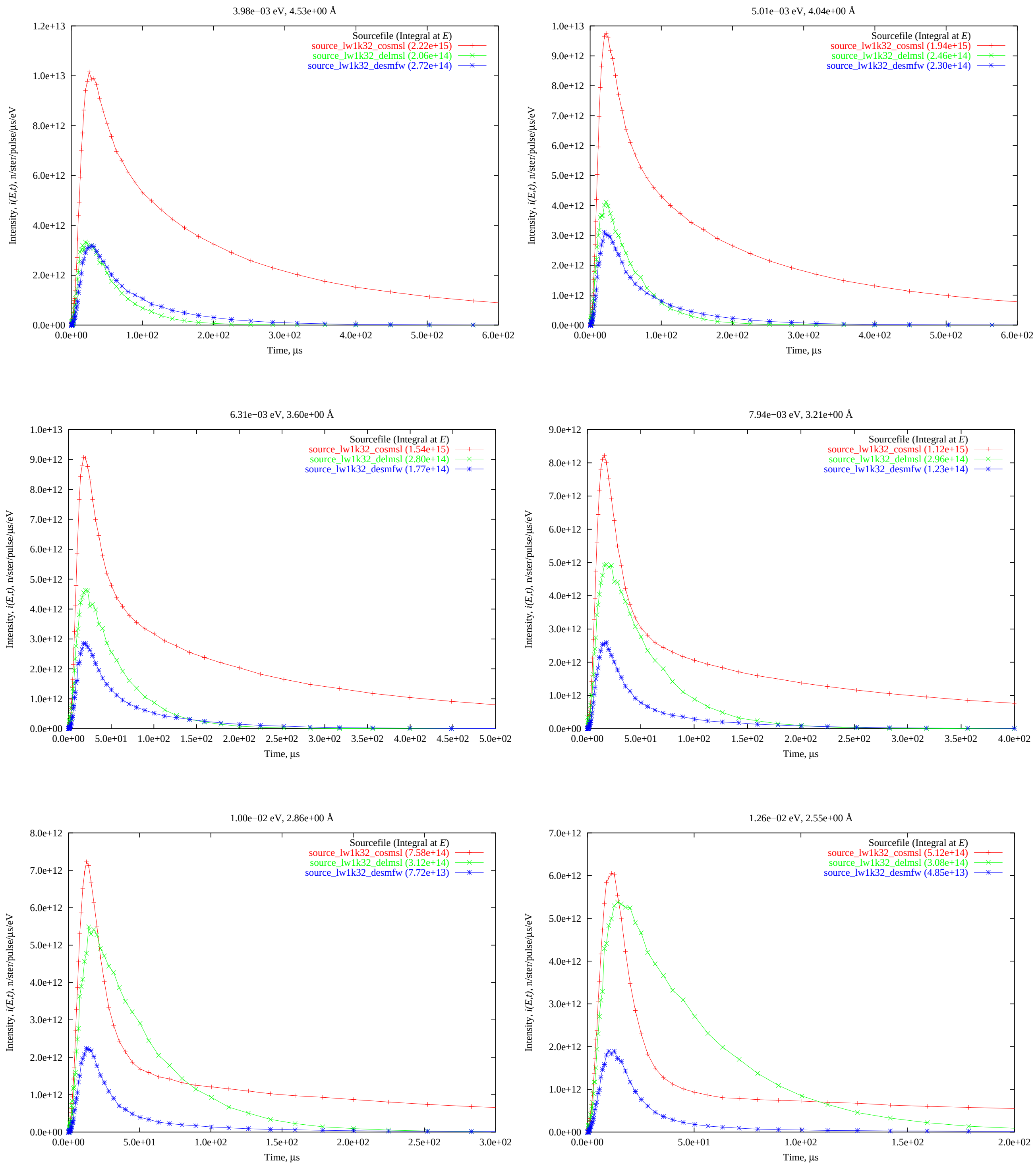

Figure 7: Emission time distributions. The coupled moderator is denoted source_lw1k32_cosmsl, the decoupled liquid methane slab moderator source_lw1k32_delmsl, and the decoupled solid methane front wing moderator source_lw1k32_desmfw. $\Delta E/E \approx 23$ %. Recall that slab moderators must be viewed indirectly.

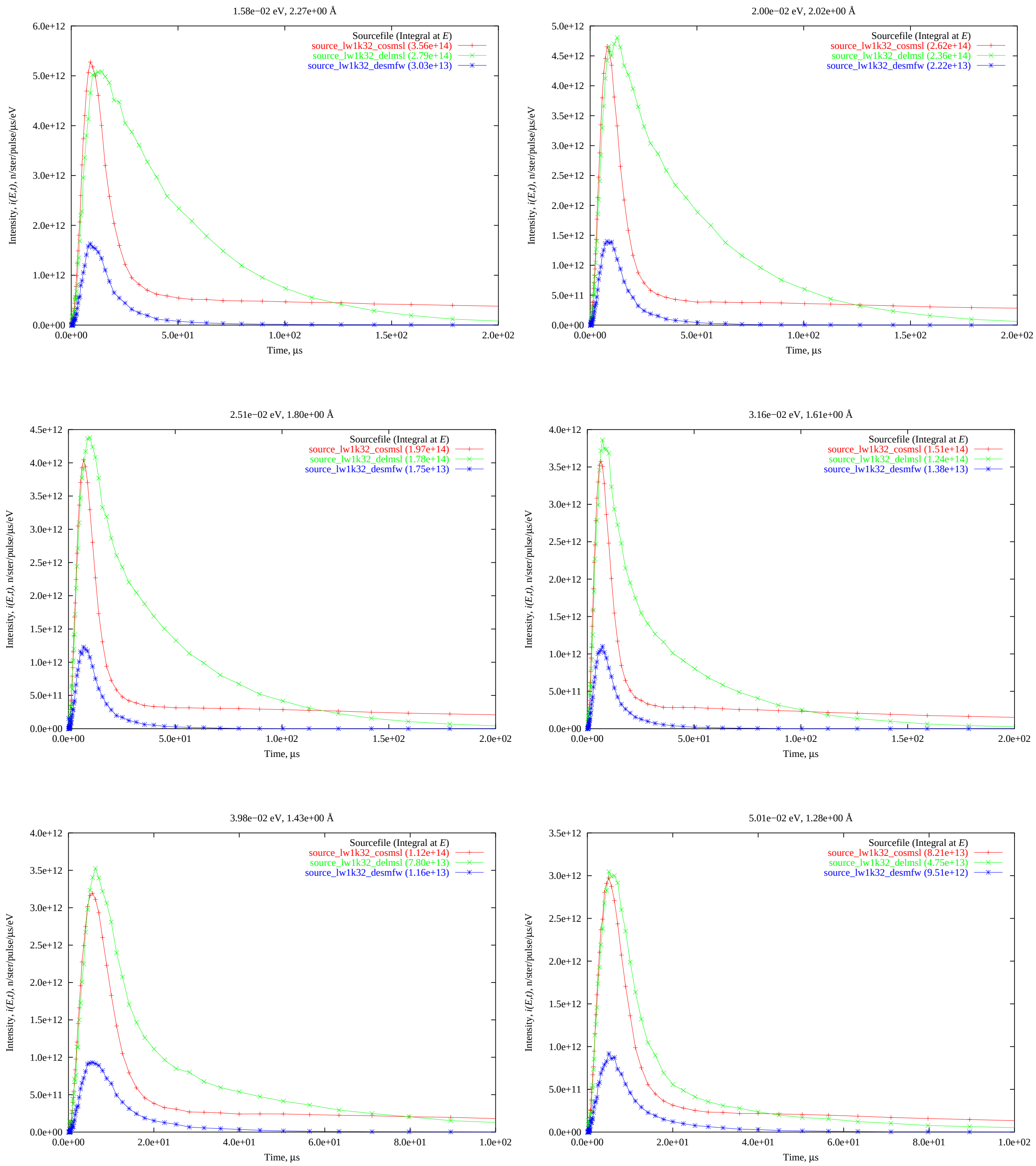

Figure 8: Emission time distributions. The coupled moderator is denoted source_lw1k32_cosmsl, the decoupled liquid methane slab moderator source_lw1k32_delmsl, and the decoupled solid methane front wing moderator source_lw1k32_desmfw. $\Delta E/E \approx 23$ %. Recall that slab moderators must be viewed indirectly.

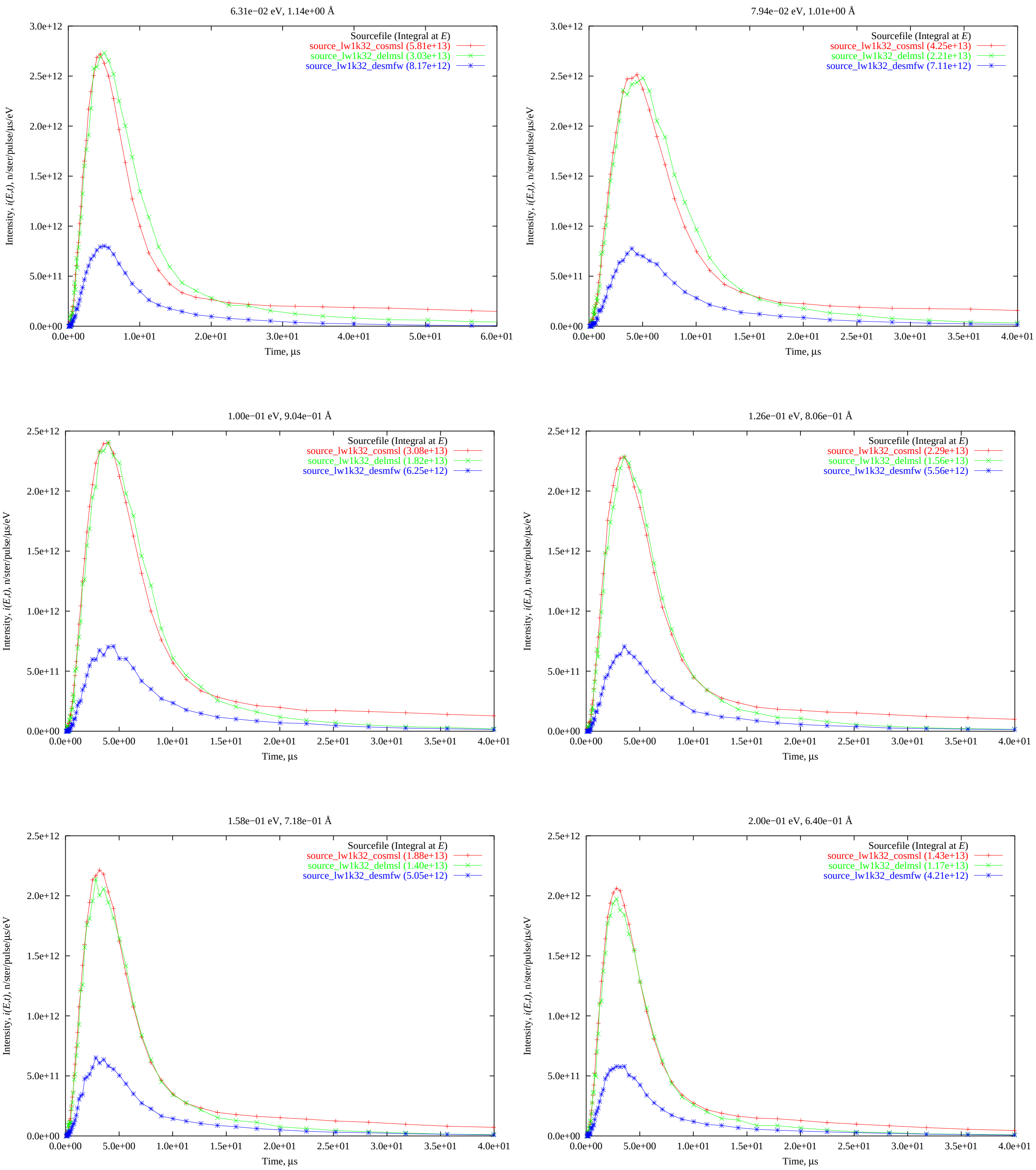

Figure 9: Emission time distributions. The coupled moderator is denoted source_lw1k32_cosmsl, the decoupled liquid methane slab moderator source_lw1k32_delmsl, and the decoupled solid methane front wing moderator source_lw1k32_desmfw. $\Delta E/E \approx 23$ %. Recall that slab moderators must be viewed indirectly.

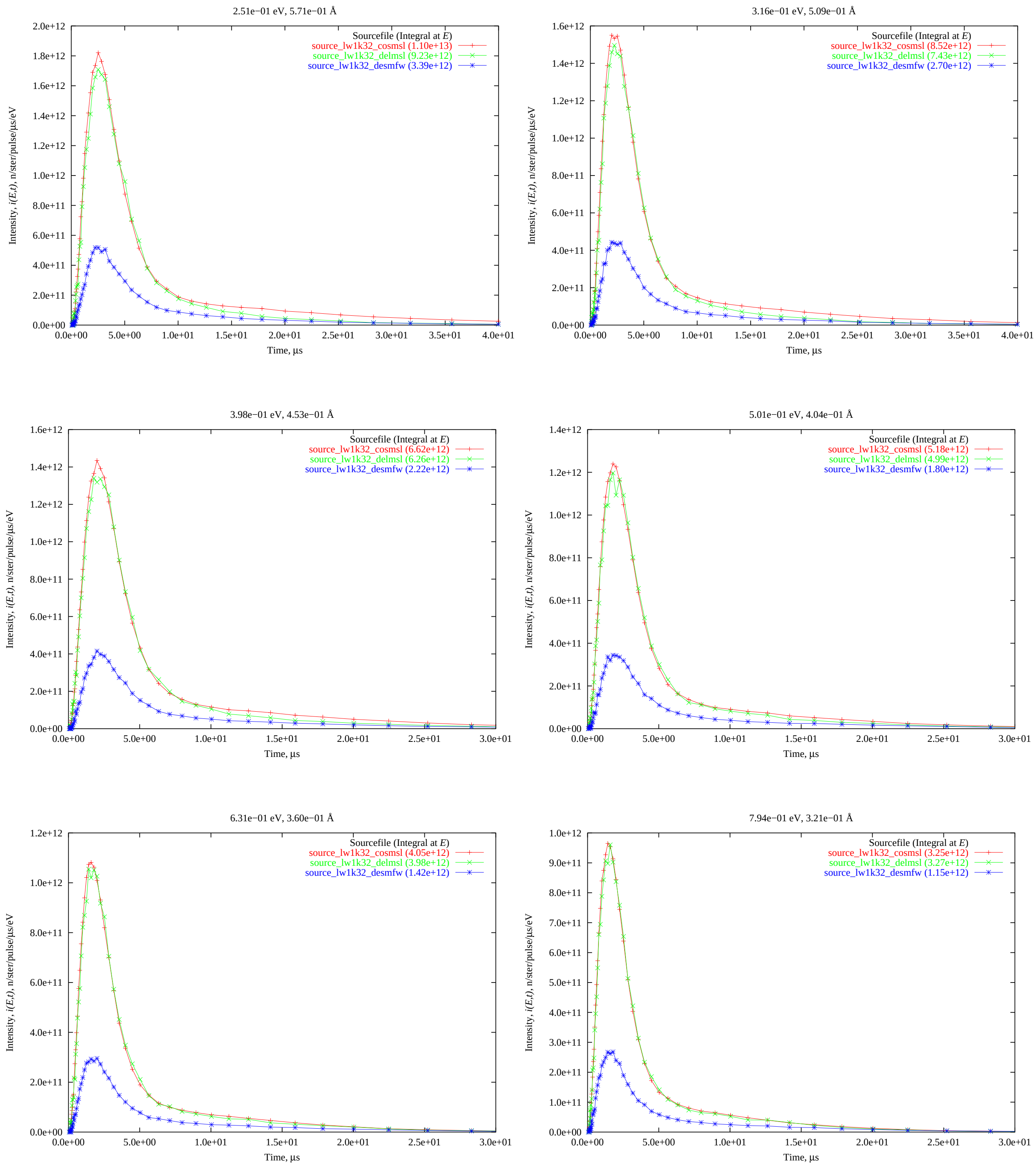

Figure 10: Emission time distributions. The coupled moderator is denoted source_lw1k32_cosmsl, the decoupled liquid methane slab moderator source_lw1k32_delmsl, and the decoupled solid methane front wing moderator source_lw1k32_desmfw. $\Delta E/E \approx 23$ %. Recall that slab moderators must be viewed indirectly.

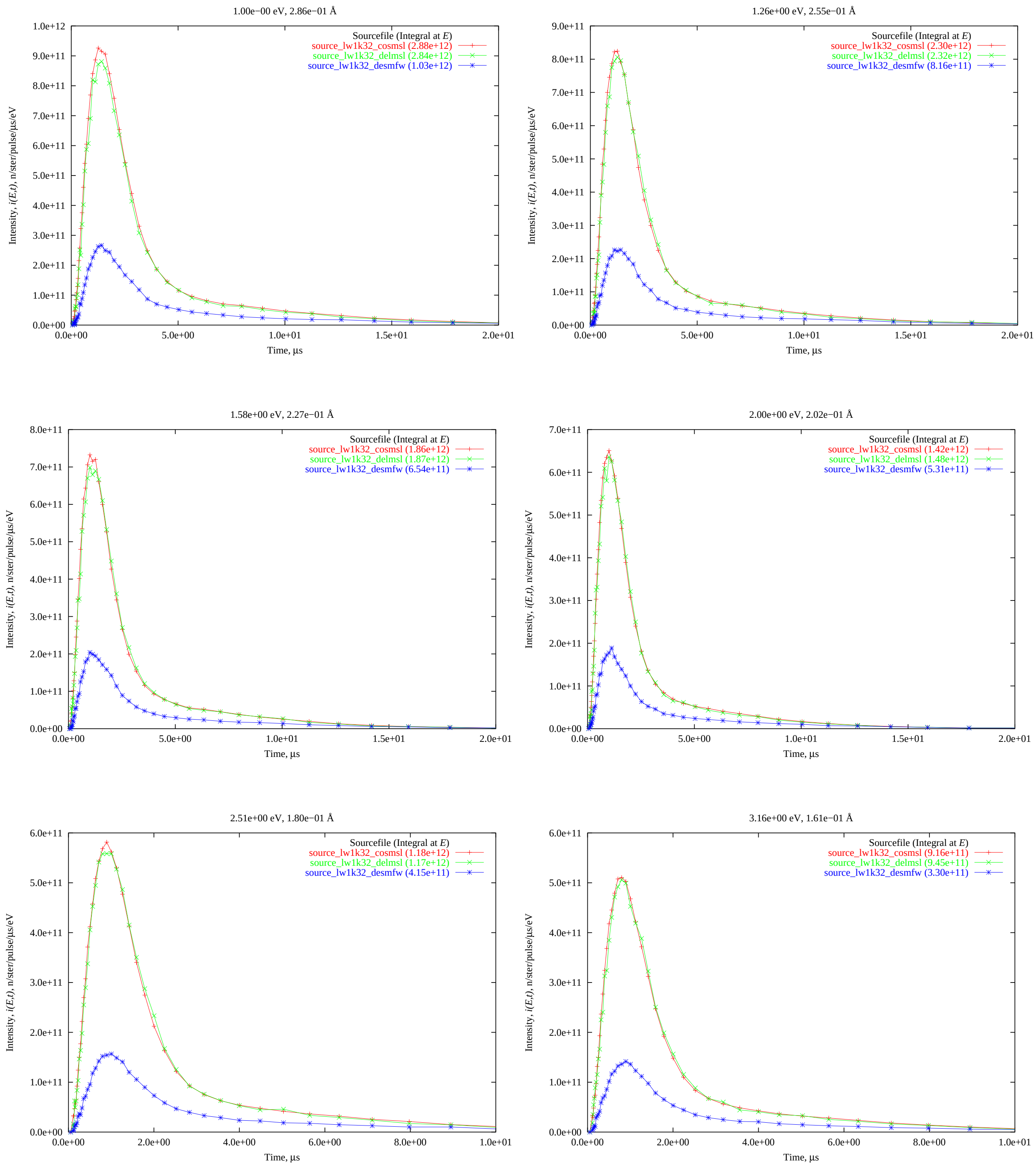

Figure 11: Emission time distributions. The coupled moderator is denoted source_lw1k32_cosmsl, the decoupled liquid methane slab moderator source_lw1k32_delmsl, and the decoupled solid methane front wing moderator source_lw1k32_desmfw. $\Delta E/E \approx 23$ %. Recall that slab moderators must be viewed indirectly.

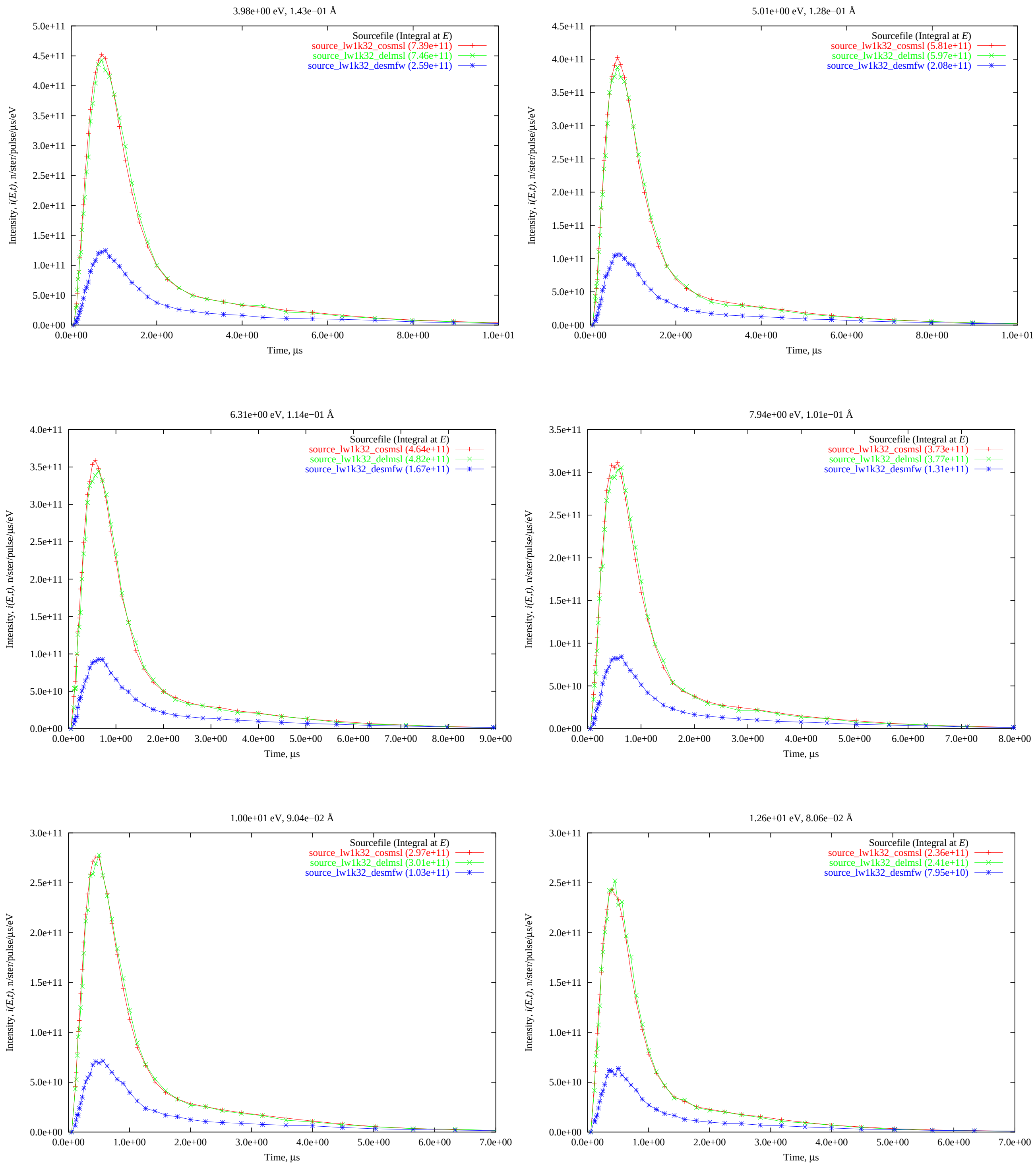

Figure 12: Emission time distributions. The coupled moderator is denoted source_lw1k32_cosmsl, the decoupled liquid methane slab moderator source_lw1k32_delmsl, and the decoupled solid methane front wing moderator source_lw1k32_desmfw. $\Delta E/E \approx 23$ %. Recall that slab moderators must be viewed indirectly.

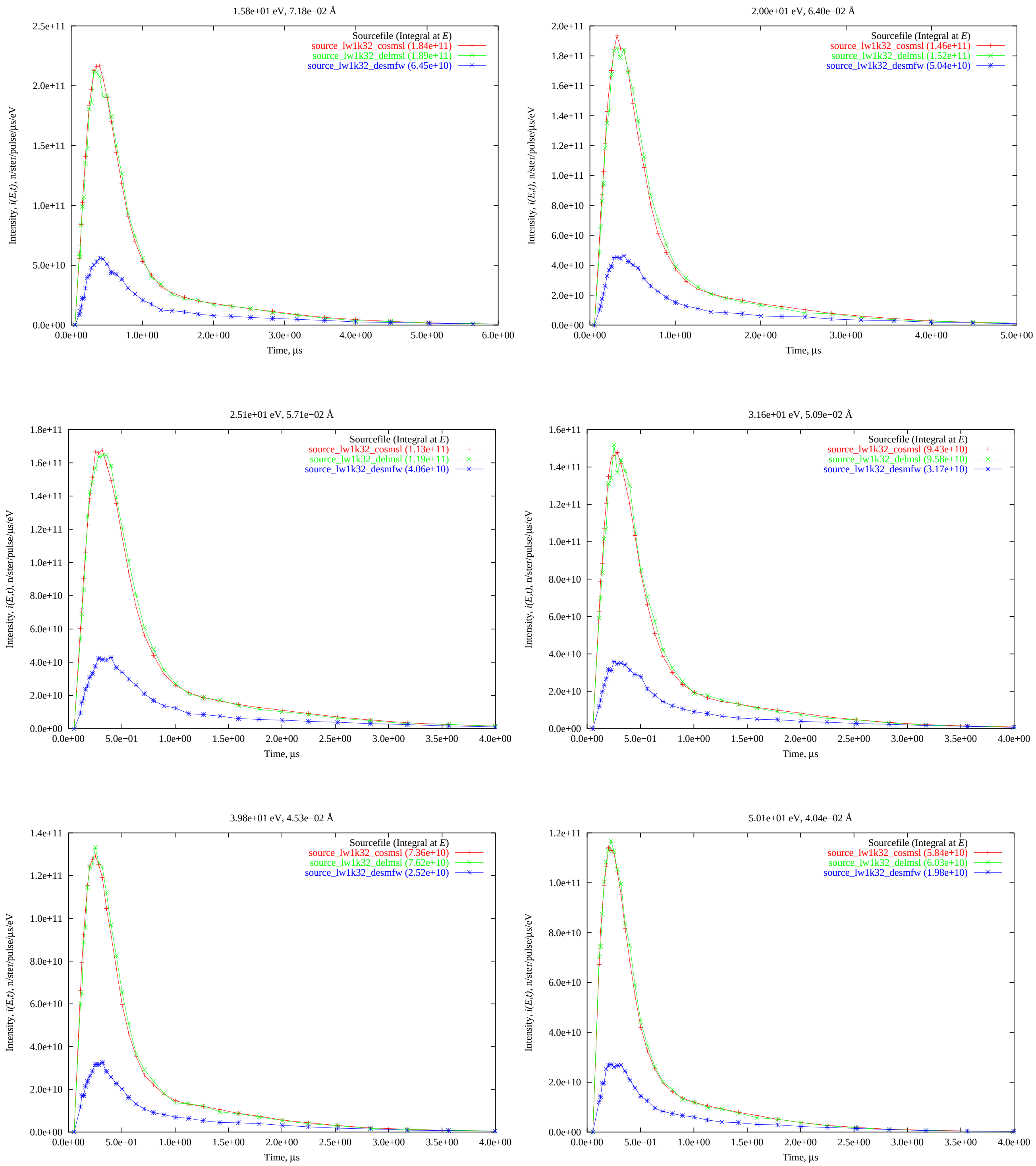

Figure 13: Emission time distributions. The coupled moderator is denoted source_lw1k32_cosmsl, the decoupled liquid methane slab moderator source_lw1k32_delmsl, and the decoupled solid methane front wing moderator source_lw1k32_desmfw. $\Delta E/E \approx 23$ %. Recall that slab moderators must be viewed indirectly.